ANL-7767

Argonne National Laboratory

CHEMICAL ENGINEERING DIVISION
FUEL CYCLE TECHNOLOGY QUARTERLY REPORT
October, November, December 1970

by

D. S. Webster, A. A. Jonke, G. J. Bernstein,
N. M. Levitz, R. D. Pierce,
M. J. Steindler, and R. C. Vogel

Printed in the United States of America
Available from
National Technical Information Service
U.S. Department of Commerce
5285 Port Royal Road
Springfield, Virginia 22151
Price: Printed Copy $3.00; Microfiche $0.95

ANL-7767
Chemical Separations Processes
for Plutonium and Uranium

ARGONNE NATIONAL LABORATORY
9700 South Cass Avenue
Argonne, Illinois 60439

CHEMICAL ENGINEERING DIVISION
FUEL CYCLE TECHNOLOGY QUARTERLY REPORT

October, November, December 1970

by

D. S. Webster, A. A. Jonke, G. J. Bernstein,
N. M. Levitz, R. D. Pierce,
M. J. Steindler, and R. C. Vogel

January 1971

Previous reports in this series: ANL-7735
ANL-7755

TABLE OF CONTENTS

LIST OF FIGURES

LIST OF TABLES

FUEL CYCLE TECHNOLOGY QUARTERLY REPORT

October, November, December 1970

by

D. S. Webster, A. A. Jonke, G. J. Bernstein,
N. M. Levitz, R. D. Pierce,
M. J. Steindler, and R. C. Vogel

ABSTRACT

During the period October through December 1970, work was done in the following areas: (1) further development of a head-end process for removing stainless steel cladding in a zinc bath by study of decladding rates, fission gas behavior, and reduction of declad fuel oxide, (2) investigation of a procedure for separating stainless steel cladding from fuel oxide by melting the cladding, (3) further laboratory-scale work to develop a fluid-bed process for the conversion of uranyl nitrate and plutonium nitrate in nitric acid solutions to an oxide form (UO_2-PuO_2) suitable for the fabrication of fuel shapes for LMFBR fuel, (4) additional development of X-ray fluorescence spectrometry as an in-line analytical method for determining the Pu/U ratio of oxide fuels during fabrication, and (5) continued investigation of the performance characteristics of a centrifugal contactor for the plutonium isolation steps in the solvent extraction of LMFBR fuels.

SUMMARY

I. Liquid Metal Decladding of Reactor Fuel

Head-end processing of LMFBR fuel will include fuel-subassembly handling, removal of stainless steel cladding and subassembly hardware from the fuel, removal of iodine and other gases from the fuel, and feeding of fuel to a nitric acid dissolution step for subsequent aqueous processing. Early LMFBR fuel elements will consist of mixed uranium and plutonium oxides jacketed in stainless steel cladding. Two decladding procedures were being studied this quarter:

1) Dissolution of stainless steel components by submerging most of the fuel subassembly in molten zinc at 800°C, separation of the zinc-stainless steel solution from the unaffected oxide fuel, and chemical reduction of the uranium-plutonium oxide to metal by contacting it with a molten metal-salt system for subsequent feeding to an acid dissolution step.

2) Melting the stainless steel cladding and draining it from the fuel (to be followed by feeding of the fuel oxide to a voloxidation or acid dissolution step).

Engineering Development of Zinc Decladding

Zinc Decladding Kinetics. Additional analytical data from decladding rate studies reported earlier confirm that the penetration rate of type 304 stainless steel by zinc at 800°C is influenced primarily by the nickel content of the zinc. The penetration rate becomes zero at a nickel concentration in the decladding solution of about 10 wt %. In the presence of high concentrations of nickel, a nickel-bearing phase precipitates, and the solubilities of iron and chromium in the zinc decladding solutions apparently decrease.

Gas-Release Experiments. To evaluate potential problems when fission-product gas is released from fuel elements during zinc decladding, three experiments were performed in which the escape of about 25 cm^3 of pressurized argon from simulated fuel elements immersed in zinc or water was observed. In two of the experiments, gas was released from 1 or 2 tubes in a bundle of 15 other simulated fuel elements fastened inside a 2-in.-ID steel shroud. The degree of splashing in this series of experiments was highly dependent on the rate of gas release. In production-scale decladding, it is expected that nearly all splashing would be confined to the interior of the subassemblies, but it is thought that even the most violent splashing could be readily deflected back into the zinc pool by means of properly designed heat shields above the zinc pool.

Reduction of UO_2 Pellets. It is proposed that zinc decladding be followed by a fuel reduction step to liberate and allow collection of the iodine and other fission-product gases and to convert the metallic uranium and plutonium to a liquid metal solution for ease in handling. Although a Mg-Cu-Ca/$CaCl_2$-CaF_2 reduction system developed for the Salt Transport Process would perform well, substitution of zinc for copper in the present application would be attractive, allowing subsequent removal of the solvent metals by evaporation. Two different Mg-Zn systems were tested: (1) Zn-30 at. % Mg, evaluated for use when dissolution of both reduced plutonium and reduced uranium in the liquid alloy is required and (2) Mg-20 at. % Zn for dissolution of only reduced plutonium. Both alloys, with and without added calcium, are being evaluated for the reduction of sintered UO_2 pellets. In two runs in which calcium was present, reduction by each Mg-Zn alloy was apparently satisfactory. In three reduction runs with Mg-20 at. % Zn alloy and with calcium absent, reduction was not complete; a portion of unreduced UO_2 covered by precipitated uranium was unavailable for reduction. Reduction with Zn-30 at. % Mg alloy in the absence of calcium has not yet been tested, but reduction runs are planned to evaluate that alloy and to confirm that good reductions can be obtained with the two Mg-Zn-Ca alloys.

Process Demonstration Experiments

Experimental apparatus has been assembled for zinc decladding experiments with 100 g of irradiated UO_2-PuO_2 fuel. Shakedown runs are nearly complete, and experiments in the shielded hot cell are to begin soon.

Melt Decladding

A series of experiments has been started to investigate the separation of fuel oxide from stainless steel cladding by melting the cladding and draining it away from the fuel. The feasibility of the procedure depends on sufficient exposure of the oxide surface as a result of drainage of the steel so that in the following step the oxide can be completely separated from the steel by either acid dissolution or voloxidation.

In five experiments, small bundles of clad UO_2 pellets (and in the first two experiments UO_2 pellet pieces) were heated above 1450°C. In one run, 1/16-in. holes in the bottom of the crucible allowed steel drainage; in the other runs the bundle was placed on the interior crucible wall at a 10° incline to allow the steel to flow to the bottom of the crucible when it became molten. Separation of steel and UO_2 was incomplete, and wetting of the UO_2 by the steel was evident; however, preliminary results indicate that in each experiment the oxide was sufficiently declad so that it would be accessible to the acid.

II. Continuous Conversion of U/Pu Nitrates to Oxides

A continuous fluidized-bed process is under development for converting uranyl nitrate-plutonium nitrate solutions to an oxide form suitable for LMFBR fuel cycle applications. Denitration produces UO_3-PuO_2 and is followed by reduction with hydrogen to yield UO_2-PuO_2, the required form for fuel manufacture. Also under consideration is the denitration of plutonium nitrate solutions alone. An integrated program of laboratory and engineering studies is in progress.

Laboratory Program

Laboratory work explored the preparation of UO_2-20% PuO_2 pellets and preliminary characterization of the pellets after sintering. The starting material was UO_3-PuO_2 powder prepared earlier in dropwise denitration experiments at 300°C, simulating the fluid-bed denitration step. Six-gram batches of powder were reduced with hydrogen in two boat experiments, one conducted at 500°C and the other at 550°C. In each experiment, the reduction time was 4 hr, and the hydrogen flow rate was 100-200 cm^3/min.

Five pellets were formed from this UO_2-PuO_2 powder. All pellets were final-pressed at 87,000 psi, but the preparation procedure for two pellets included prepressing at ∿1500 psi, then granulating to pass through a 45-mesh screen. After pressing, sintering was at 1650 or 1750°C for 1 1/2 or 4 hr. Pellet diameters were ∿0.25 in., and pellet lengths were 0.1 to 0.3 in. Pellet densities ranged from 83 to 89% of theoretical.

Examination of pellets by several techniques resulted in the following observations. Electron microprobe scanning of a section of a UO_2-20 wt % PuO_2 pellet that had a density of 84% of theoretical showed good homogeneity. Chemical analysis of this pellet indicated an oxygen/metal (O/M) atom ratio of 1.98. A single set of X-ray diffraction lines was found, indicating the presence of a single oxide phase.

Apparatus has been set up for measuring the solubility of uranium-plutonium nitrate in dilute nitric acid solutions. From this information, the practical limits of concentration of U/Pu nitrate solutions for feeds to the denitration process will be determined; high concentrations are desired to maximize throughput. Equipment checkout tests have been performed in which crystallization temperatures were determined from cooling curves for uranyl nitrate solutions. Results agree with published data. These tests will be followed by experiments with uranium-plutonium solutions.

Engineering Program

The operability of a fluid-bed denitration pilot plant was previously demonstrated in shakedown runs with uranyl nitrate. These runs were done with the auxiliary process vessels on hand, pending a criticality review for operation with plutonium-containing feeds. The pilot plant is now being modified to meet criticality requirements for work with uranyl nitrate-plutonium nitrate solutions.

III. In-Line Analysis in Fuel Fabrication

X-ray fluorescence is being evaluated as a direct in-line analytical method for determining plutonium/uranium ratio in uranium-plutonium oxide, which is expected to be the fuel for the first commercial fast breeder reactor. Initial work is with ThO_2-UO_2 as a stand-in for UO_2-PuO_2. The use of a newly designed sample holder was shown to decrease analysis time and to improve precision. In other work, it was observed that fluorescence intensity decreases for particles of 44 μm or larger. It has been concluded that this nondestructive analysis can be performed rapidly enough for large-scale processing.

IV. Adaptation of Centrifugal Contactors in LMFBR Fuel Processing

A centrifugal contactor of small diameter and large length-to-diameter ratio is being studied to extend centrifugal contactor design to a configuration suitable for plutonium isolation steps in the solvent extraction of LMFBR fuels. Fabrication of a stainless steel contactor patterned after units in use at Savannah River is nearing completion. In the Savannah River contactor, aqueous and organic streams are mixed by a paddle in a mixing chamber at the bottom of the contactor. The mixer also acts as a centrifugal pump, discharging the mixed phases into the bottom of a hollow rotor bowl.

Mixing in the contactor being fabricated here is with a removable paddle and mixing chamber. However, this contactor can be modified so that the aqueous and organic streams are mixed as they move downward in the annular space between the spinning rotor and the stator or casing. The manner whereby the phases are separated following mixing is identical. The mixture enters an orifice in the bottom of the hollow rotor, and the phases are separated as they move upward inside the rotor.

A plastic contactor was built for preliminary testing to evaluate some of the operating characteristics of the annular mixer design. These tests showed high mixing power input and good throughput capacity when a single liquid phase was fed. When the contactor was operated with aqueous

and organic phases, the aqueous phase outflow stream was observed to be contaminated with organic phase. A series of tests was made to establish the cause of this deficiency. Apparently, hairline cracks in the plastic weir tube for the organic phase permitted a small quantity of separated organic phase to flow into the aqueous phase outflow stream. Since most of the goals sought by operation of the plastic unit were reached, no further runs with the plastic contactor are planned. Additional testing of the annular mixing concept will be made with the stainless steel contactor.

I. LIQUID-METAL DECLADDING OF REACTOR FUELS

(R. D. Pierce)

Liquid-metal decladding processes under development at Argonne appear to provide relatively simple and inexpensive techniques for solving formidable head-end processing problems related to the high burnups, short cooling times, residual sodium, and high plutonium content of irradiated LMFBR fuels.

Early LMFBR fuel elements will consist of mixed uranium and plutonium oxides jacketed in stainless steel tubes. These fuels may be irradiated to burnups up to 100,000 MWd/ton at specific powers as high as 175 kW/kg and may be allowed to decay for only 30 days. The localized heat emission of LMFBR fuels is very high, creating heat-dissipation problems during handling and processing operations.

High concentrations of radioactive iodine (especially ^{131}I), xenon, and krypton in spent LMFBR fuel will present serious problems in handling and disposing of the waste-gas effluent from reprocessing operations. To avoid excessive emissions of highly radioactive isotopes such as ^{131}I to the environment, head-end operations must be performed in a sealed cell, and fission gases must be efficiently contained. If possible, the volatile elements should be removed from the fuel material prior to the nitric acid dissolution step of aqueous fuel processing.

If sodium is present in failed fuel elements, it too could present cleaning and fuel-dissolution problems since sodium can react explosively with nitric acid. In addition, the high plutonium content of LMFBR fuel presents severe criticality problems.

In one scheme for liquid-metal decladding, cladding is removed by immersing all of the fuel region of a discharged fuel subassembly (probably after cropping the bottom) in a pool of molten zinc having a molten-salt cover layer. The zinc dissolves the stainless steel components (i.e., the subassembly supporting members and the cladding), but does not react with the fuel oxides. The resulting solution is then separated from the fuel oxides.

Advantages of liquid-metal decladding include (1) efficient removal of iodine and other volatile fission products, (2) relative ease of dissipation of fission-product heat, (3) elimination of the requirement for separate sodium-removal steps, (4) discharge of all process waste streams (except Xe and Kr) as solids having good heat-transfer properties, (5) collection of xenon and krypton in an inert cover-gas mixture (containing ~50% Xe plus Kr) of small enough volume to allow storage in gas cylinders, (6) absence of effective neutron-moderating elements, and (7) process simplicity and flexibility.

The principal disadvantages of liquid-metal decladding are a lack of industrial experience in the use of refractory metals and graphite as materials of construction, and the need to dispose of large quantities of reagent zinc as waste. Although refractory metals and graphite are compatible

with liquid zinc and molten salts and equipment fabricated of these materials have long lives, their cost is a significant portion of the processing cost. About 20 ft^3 of zinc is used for each ton of fuel processed. However, solid zinc is an ideal waste form, and the reagent and waste-disposal costs are not large. An alternative to zinc storage is recovery of the zinc by a zinc-vaporization process.

Another scheme for liquid-metal decladding is direct melting of the stainless steel cladding. A major portion of the molten steel can be separated from the fuel and cast into a waste ingot; the steel still associated with the fuel can be charged with the fuel to either an acid dissolution step or a voloxidation step to complete the separation of steel from fuel. Melt decladding avoids mechanical dismantling of the fuel, allows fission gases to be collected in a compact form, evaporates residual sodium from the fuel, provides a compact waste, and adds no extraneous metal to the fuel before it is fed to the acid dissolution step. The major difficulties of the step are high temperature (>1450°C), relatively poor separation of steel and oxide, difficulties in handling the declad fuel, and low removal of iodine from the fuel.

A. Engineering Development of Zinc Decladding

The effects of stainless steel and nickel concentrations in a zinc decladding melt on decladding rates are being studied.

Experiments have been performed simulating the release of high-pressure gas inside the shroud of a cropped fuel subassembly upon rupture of the cladding of a fuel element immersed in a zinc melt.

A step proposed to follow liquid-metal decladding is reduction, in which declad oxide is reduced to metal by contacting with a liquid salt and a molten alloy containing a reductant. Experiments are being performed to study the reduction of sintered UO_2 pellets with a liquid halide salt mixture and one of the alloys, Mg-20 at. % Zn, Mg-17 at. % Zn-4 at. % Ca, Zn-29 at. % Mg-6.6 at. % Ca, and Zn-30 at. % Mg.

1. Zinc Decladding Kinetics (T. R. Johnson, I. O. Winsch, J. J. Stockbar, T. F. Cannon, R. W. Clark)

Steel dissolution in zinc at 800°C has been found to be rapid, and stainless steel loadings of 26% have been achieved. Information obtained on the kinetics of steel dissolution in zinc provides a basis for the engineering design of the process. The highlights of decladding kinetics investigations at Argonne between early 1968 and early 1970 have been summarized (ANL-7735, pp. 15-20). In two recent experiments (ZDS-12 and 13), the relative rates of dissolution and penetration at 800°C of type 304 stainless steel tubes by zinc containing known concentrations of nickel and stainless steel was studied (ANL-7755, pp. 8-14). The test procedure was as follows. The stainless steel tube was exposed for the specified time in a Zn-Fe-Cr-Ni melt, and then removed for vacuum retorting, weighing, and metallographic examination. Sufficient stainless steel or nickel was then added to the melt to bring it to the next desired composition. Results indicated that the penetration rate is primarily related to the nickel content of the liquid zinc phase.

In run ZDS-13 with zinc solutions saturated with iron and chromium, the rate of attack was measured for nickel additions equivalent to concentrations of 5 to 13 wt %. As reported in ANL-7755, p. 9, the final liquid phase in run ZDS-13 was calculated to contain 5.8 wt % Fe, 1.0 wt % Cr, and 12.8 wt % Ni, based on the assumptions that all of the nickel added was in the liquid phase, that the cosolubilities of iron and chromium in zinc at 800°C are 5.8 wt % and 1.0 wt %, respectively, and that the solid phase in equilibrium with the saturated zinc solution contains 45 wt % zinc. However, analysis of a filtered sample taken at the end of ZDS-13 was approximately 3 wt % Fe, 0.6 wt % Cr, and 8.5 wt % Ni, in disagreement with the calculated values. Analytical results have subsequently been received for a sample taken at the same time as the first sample. There is substantial agreement with the earlier analytical results. Evidently, in the presence of nickel, the cosolubilities of iron and chromium are lower than their individual solubilities, and the solid Zn-Fe-Cr phase that precipitates contains considerable nickel.

This result does not change the qualitative conclusions concerning the dissolution mechanism, i.e., that the steady-state penetration rate of zinc into type 304 stainless steel is influenced primarily by the nickel content of the solution, and that the iron and chromium contents of the solution influence the initial penetration rate (during the first 5 min of immersion)--primarily by affecting the thickness of the adhering solid reaction layer. The new data indicate a different quantitative relationship of penetration rate to nickel content. The penetration rate can be described as being linearly dependent on nickel concentration rather than dependent on the square of the nickel concentration (as reported earlier). A zero penetration rate at a nickel concentration of about 10 wt % is predicted; in comparison, the nickel solubility in zinc is 12 wt % at 800°C.[1]

This reassessment of the experimental kinetic data does not alter the process design concepts. Although dissolution and penetration of stainless steel by zinc are not completely understood, the level of understanding seems adequate for the present preliminary design work.

2. Gas-Release Experiments (I. O. Winsch, T. F. Cannon, J. J. Stockbar)

Three experiments have been performed simulating the release of high-pressure gas from fuel elements during zinc decladding. The tentative procedure for zinc decladding of fuel subassemblies is immersion of all of the fuel portion of a cropped fuel subassembly in the melt to completely remove cladding from the fuel-containing sector of the fuel elements. The fission-product gases will escape from the plenum region of the fuel elements and will bubble through only shallow layers of zinc and salt.

An earlier report (ANL-7755, pp. 21-22) described the release of gas into a zinc-salt melt from two simulated fuel elements pressurized with argon to a 54-atm pressure[2] and attached inside a 2-in.-dia stainless steel shroud. In that experiment, the shroud was sealed except for a 5/8-in.-dia hole in the bottom, and the depth of immersion of the stainless steel tubes simulating fuel elements was 3 in. Some zinc was splashed out of the containment vessel by the escape of gas from the bottom of the shroud.

In three recent experiments, 2, 17, and 17 simulated fuel elements were contained in the simulated subassemblies. The 2-in.-dia stainless steel shroud for the first experiment had a 5/8-in.-dia opening in the bottom and six 1/4-in. dia vent holes spaced around the circumference, 11 in. above the shroud bottom. These holes provided a means of equalizing the pressure inside and outside the tube. Two type 304 stainless steel tubes (1/4-in. OD by 0.010-in. wall) were pressurized to 52 atm with argon, and a valve leading to the argon supply was closed. The assembly of simulated shroud and fuel elements was immersed in a zinc-salt melt at 808°C to a depth of 3 in. The pressure rose to 55.5 atm; after 1.5 and 1.75 min, the gas escaped rapidly from the tubes. Examination of the tubes after the experiment revealed that steel pins that had been inserted in the tubes to represent fuel pellets had remained inside the tubes. Zinc and cover salt had splashed to a height of 37 in. inside the shroud; there was no evidence of splashing outside the shroud.

The next experiment was done with a bundle of simulated fuel elements whose packing resembled the configuration in an LMFBR fuel subassembly. Two of the simulated fuel elements in this assembly were type 304 stainless steel tubes (50 in. long, 0.25-in. OD, 0.01-in. wall) containing close-fitting steel pins (simulated fuel) in their lower portions and pressurized with argon (about 50 atm). These tubes and fifteen stainless steel rods (0.25-in. dia by 37-in. long) surrounding the tubes were fastened inside a 37-in.-long, 2-in.-OD stainless steel tube representing the shroud of a fuel subassembly. The shroud was sealed at the top and had a 5/8-in. opening at the bottom and six 1/4-in. holes drilled around the circumference, 11 in. above the bottom. Each tube projected through a seal in the top of the shroud. Spacing between the mock fuel elements was achieved by winding each rod with 48-mil wire at a pitch of one turn per foot.

The simulated fuel subassembly was immersed to a depth of 3 in. into a zinc-salt melt at 800°C. The pressure inside the 1/4-in.-OD tubes rose to 55 atm; one tube ruptured after 1.87 min and gas was rapidly released; after 1.95 min, gas was rapidly released from the other tube. The furnace contents were examined after this experiment. Although zinc had splashed to a height of 20 in. in the bundle, there was no evidence that salt or metal had splashed outside the shroud. Stainless steel plugs welded into the bottoms of the 0.25-in.-dia tubes separated from the tubes during the exposure, but the simulated fuel had remained inside the tubes.

In the third experiment, tests were made to observe the effects of a sudden release of gas under pressure from tubes positioned at different locations in a simulated subassembly immersed in water. The subassembly consisted of a bundle of two tubes surrounded by 15 rods and fastened inside a 1.94-in.-ID transparent Lucite tube simulating a shroud. The shroud was open at the top and had a 5/8-in.-dia hole centered in the bottom. Each stainless steel tube (1/4 in. OD by 37 in. long) was crimped at the lower end, leaving an opening of about 0.004 $in.^2$ Each rod had a 1/4-in. OD and 37-in. length. The subassembly was immersed to a depth of 4 in. in water, and argon was fed to the tops of the tubes by opening valves to a manifold containing argon under pressure. The choice of water as the liquid and of some transparent components allowed the behavior of the liquid to be observed.

The effects of sudden release of ~50 cm^3 of argon at 52-atm pressure through the small openings in one or both tubes were observed. When gas at 52-atm pressure was released from tubes located over the opening in the bottom of the shroud, gas was blown out of the bottom of the shroud and water splashed out of the container. When gas at 52-atm pressure was released from tubes located near the wall of the shroud, little gas escaped from the shroud, but the water level in the shroud rose to about 37 in. when both tubes were vented. Less displacement would be expected in a run with zinc.

Based on the observations made in these scouting experiments, it appears that zinc splashing may occur during zinc decladding but would be confined largely to internal spaces in fuel subassemblies. It is thought that the most violent splashing outside the subassemblies would be contained adequately by heat shields above the melt, which would be designed to function also as deflectors. No additional gas-release experiments are planned at this time, but information obtained during fuel examination (by other investigators) on the behavior of fission-product gases when irradiated fuel elements are perforated will be sought and evaluated.

3. Reduction of UO_2 Pellets (I. O. Winsch, T. F. Cannon, J. J. Stockbar)

It has been proposed (ANL-7735, pp. 26-32) that removal of stainless steel cladding by a liquid-metal decladding step be followed by reduction of the oxide to metal in the decladding vessel. An advantage of this procedure would be that all iodine would be released and collected in the waste salt and all volatile fission products (ANL-7755, pp. 24-31) would be released inside the decladding vessel and could be collected for storage with minimum dilution by other gases (ANL-7735, pp. 32-33; ANL-7755, pp. 32-33).

In the proposed reduction step, declad oxide fuel is contacted with a liquid salt and a molten-metal alloy containing a reductant. With adequate mixing (stirring) of the fuel oxide, salt, and metal, reaction with the reductant completely converts the uranium oxide and plutonium oxide to metal. Depending on which molten metal is employed, both uranium and plutonium may be extracted into the molten metal phase (which separates from the salt and may be pressure-siphoned out of the reaction vessel) or the reduced uranium may be in the form of a precipitate with only the plutonium going into solution. In the latter procedure, an additional uranium dissolution step is required (e.g., a step in which a liquid U-Fe alloy is formed) followed by pressure-siphoning of the uranium solution out of the reaction vessel.

After the fuel (in solution in a large quantity of alloy) is removed from the crucible, it is dissolved in nitric acid for aqueous solvent-extraction processing. Alternatively, if the metals used in the reduction step are volatile (e.g., magnesium and zinc), these metals may be removed by retorting before the acid dissolution step and recycled through the process.

A metal-salt system developed for the Salt Transport Process, which results in excellent reduction of uranium and plutonium, consists of calcium dissolved in Mg-42 at. % Cu and a $CaCl_2$-CaF_2 salt (ANL-7735, pp. 21-25). In

a limited number of runs, two alternative alloys, which could be recovered by evaporation and recycled, are being evaluated for this system. They are (1) Zn-30 at. % Mg, which would give a product solution containing reduced uranium and plutonium, and (2) Mg-20 at. % Zn, which would give a product solution containing only reduced plutonium. Runs are being made with and without calcium added to the alloy.

Experiments are being performed, using sintered UO_2 pellets (0.21-in. dia, 0.25 in. long), to study the reduction of UO_2. Experience has shown that $(U,Pu)O_2$ and PuO_2 are easier to reduce than UO_2. In run Mg-Zn-R1, the charge was 1 kg of pellets, and the reduction step was performed in a baffled tungsten vessel (10 5/8-in. ID and 19 in. high) equipped with an agitator. The charge for each subsequent experiment was 200 g UO_2. Runs Mg-Zn-R2 through -R5 were performed in an inductively heated tilt-pour furnace using a baffled tungsten vessel (5 3/4-in. OD, 5 1/2-in. ID, 13 7/8 in. high). A Mo-30 wt % W agitator (3-in. dia, 1 1/4-in.-wide blade pitched 30° from horizontal, deflecting downward) was used to mix the melts at 900 rpm during reduction of UO_2. The reduction temperature was 800°C in all experiments. Run durations were 5, 5, 1, 1, and 5 hr for experiments Mg-Zn-R1 through Mg-Zn-R5, respectively.

The alloy charged in experiments Mg-Zn-R1 to -R3 was Mg-20 at. % Zn, and the salt was $MgCl_2$-47.5 mol % $CaCl_2$-5 mol % CaF_2. Reduction to uranium metal was nearly complete in these three experiments, except that a large amount (10 to 20%) of the UO_2 was engulfed by the precipitating uranium and not available for reduction. This UO_2 was recovered after the uranium precipitate was dissolved in Zn-30 at. % Mg for analytical purposes.

In runs Mg-Zn-R4 and Mg-Zn-R5, calcium was added to the Mg-Zn alloy and $CaCl_2$-20 mol % CaF_2 was the salt phase. This metal-salt system was selected to increase the reduction rate and because it is expected to improve efficiency of plutonium extraction in future runs in which plutonium will be present. In Mg-Zn-R4, 3.39 kg of Mg-17 at. % Zn-4 at. % Ca alloy and 1.08 kg of the salt were charged; in Mg-Zn-R5, the charge was 3.55 kg of Zn-29 at. % Mg-6.6 at. % Ca and 1.08 kg of salt.

The preliminary results now available indicate that good reduction (>99%) of UO_2 pellets was obtained with Mg-17 at. % Zn-4 at. % Ca/$CaCl_2$-20 mol % CaF_2 (run Mg-Zn-R4) and with Zn-29 at. % Mg-6.6 at. % Ca/$CaCl_2$-20 mol % CaF_2 (run Mg-Zn-R5). All of the uranium was soluble in the reduction alloy used in run Mg-Zn-R5, but the solubility of uranium in the reduction alloy of run Mg-Zn-R4 was low. No UO_2 was entrapped by the precipitated uranium in run Mg-Zn-R4; the reason for the difference in UO_2 entrapment between this calcium system and the similar calcium-free system of runs Mg-Zn-R2 and -R3 is not understood at this time. Oxide fuel entrapment was never encountered with the Mg-Cu-Ca/$CaCl_2$-CaF_2 reduction system employed in studies of the Salt Transport System.

Runs are planned to verify the good results obtained with calcium in the two Mg-Zn alloys and to evaluate the system Zn-30 at. % Mg/$MgCl_2$-$CaCl_2$-CaF_2. An experiment will be made to determine the solubility of uranium in alloys of Zn-30 at. % Mg plus calcium at 800°C.

B. Process Demonstration Experiments (T. R. Johnson, W. A. Murphy, R. W. Clark)

Equipment and facilities have been prepared for small-scale (100 g UO_2-PuO_2) decladding experiments with irradiated oxide fuel. The experimental procedure will consist of the dissolution of stainless steel cladding by liquid zinc, removal of the fuel pellets from the zinc in a tantalum basket, and reduction of the fuel oxide to metal in a molten metal-salt system. The details of the experimental procedure and equipment were described in the previous report (ANL-7755, pp. 14-17).

The experimental apparatus has been assembled, shake-down runs with the equipment outside the shielded cell are nearly complete, and experiments in the cell are to begin soon.

C. Melt Decladding (I. O. Winsch, T. R. Johnson, T. F. Cannon, J. J. Stockbar)

A series of experiments has been started to investigate fuel oxide separation from stainless steel cladding by melting the cladding away from the fuel. The feasibility of the procedure depends upon sufficient exposure of oxide surface as a result of draining of the stainless steel so that the oxide can be completely separated in the following step by either acid dissolution or voloxidation.

In each experiment, the charge was melted in a magnesia or alumina crucible in an induction furnace. A charge consisted of a bundle of type 304 stainless steel tubes containing UO_2 and wrapped with 10-mil-thick type 304 stainless steel to simulate a fuel subassembly shroud. A weight ratio of uranium oxide to stainless steel of about two was selected; this is consistent with the approximate fuel-to-steel ratio for proposed LMFBR fuel which is two if the end hardware is ignored.

Five experiments (SSMD-1 to -5) were performed. In SSMD-1 and -2, stainless steel tubes (0.25-in. dia, 0.010-in. wall, 3-in. length) crimped closed at one end were charged with UO_2 pellets (0.21-in. dia, 0.25-in. length) and crushed UO_2 pellets (+14 mesh). The charges for the other experiments were similar except that crushed oxide was omitted.

The magnesia crucible used in SSMD-1 had six 1/16-in.-dia holes in its base and was positioned above a second crucible. Heating of the ~135-g charge for 1.5 hr at 1460-1608°C under vacuum caused only 12% of the stainless steel (melting range of 1400-1450°C) to flow into the lower crucible and caused 45% of the stainless steel to evaporate. In this experiment and in subsequent experiments, stainless steel had wet the UO_2. The steel remaining in the crucible was bonded to UO_2 pellets and particles in two large clusters; about one-half of the UO_2 was loose. The two large clusters were digested in 8M HNO_3, and the clusters lost 44% of their weight. All of the UO_2 was accessible to the acid. The undissolved residue was analyzed; less than 0.001% of the uranium was entrapped in the steel.

In SSMD-2 to -5, the induction furnace contained a single crucible and was tilted 10° from the horizontal. A charge was placed on the interior wall of the crucible, and it was expected that upon heating, the molten steel would flow to the bottom of the crucible and the pellets would

remain on the wall above the steel. An argon atmosphere at 630 mm Hg pressure was maintained inside the furnace. Temperatures of 1490 to 1650°C were maintained for 1 hr. Inspection of the magnesia crucible and its contents after SSMD-2 and -3 showed that most of the stainless steel had flowed away from the pellets, but that the pellets had been wet by the stainless steel. The bond strength was such that when the stainless steel and UO_2 were separated, the UO_2 fractured rather than the bond.

Figures 1 and 2 are photographs of UO_2 and steel that had been carefully removed from the crucibles after SSMD-4 and -5. In SSMD-4 and -5, Alundum crucibles were used and were charged with 162 g of UO_2 pellets and 81 g of stainless steel in an assembly of 20 simulated fuel elements. The temperature was 1490°C during SSMD-4, and 1650°C during SSMD-5. In both runs, a sizable quantity of the molten steel collected on the crucible wall above the pellets and failed to flow to the bottom of the crucible. At the lower temperature, none of the stainless steel flowed to the bottom of the crucible. In both runs, most of the pellets were loose but were wetted in spots with steel.

Several additional experiments will be made with the crucible wall positioned at a 20° angle in an attempt to cause additional stainless steel to flow downward. Also, a run will be made employing an Ar-4% H_2 atmosphere to duplicate the conditions used by Irvine of ORNL.[3,4] Irvine found that UO_2 pellets were wet little or not at all by molten stainless steel in an Ar-4% H_2 atmosphere.

Fig. 1. Contents of Crucible After Melt Decladding, SSMD-4. ANL Neg. No. 308-2423.

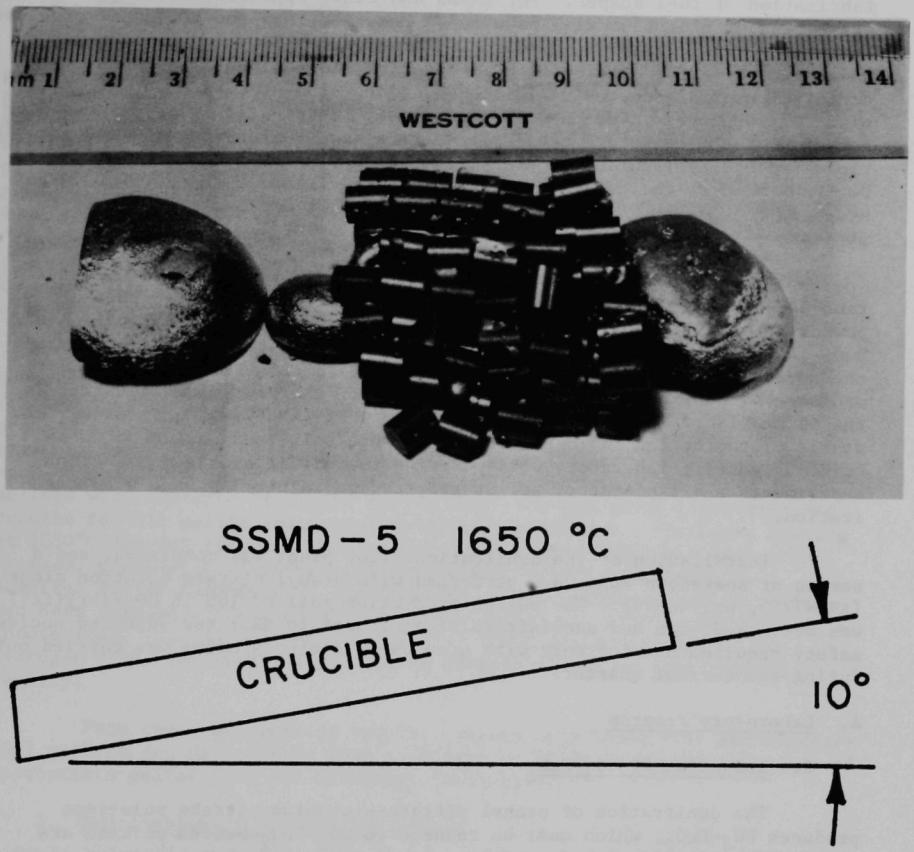

Fig. 2. Contents of Crucible After Melt Decladding, SSMD-5. ANL Neg. No. 308-2372.

II. CONTINUOUS CONVERSION OF U/Pu NITRATES TO OXIDES

(N. M. Levitz, D. E. Grosvenor, S. Vogler, F. G. Teats)

The nuclear fuel cycle requires the conversion of uranyl nitrate and plutonium nitrate solutions to powdered oxides suitable for the fabrication of fuel shapes. For LMFBR and other applications large quantities of plutonium will have to be recycled, and the attendant problems of nuclear criticality, intrinsic radiation, and safety in shipping serve as an incentive for developing high-capacity, low-holdup continuous denitration processes. A fluidized-bed conversion process under study, based on technology developed in earlier ANL fluidization work,[5] shows high potential for meeting all process requirements. Basic process steps include fluidized-bed denitration of uranyl nitrate-plutonium nitrate solutions to UO_3-PuO_2 powder, followed by fluidized-bed reduction of the UO_3-PuO_2 with hydrogen to UO_2-PuO_2. Laboratory-scale and pilot engineering work is in progress.

As reported earlier (ANL-7735, pp. 45-49), laboratory drop-denitration experiments simulating the fluidized-bed denitration step produced powder from a U-20% Pu nitrate solution which showed good distribution of PuO_2 in the UO_3 matrix. Also reported earlier (ANL-7735, pp. 49-52) was the development of a procedure for dissolution of UO_3-PuO_2 material produced by denitration to facilitate reuse of the plutonium inventory in the pilot plant. In subsequent laboratory work (ANL-7755, pp. 38-40), the stable plutonium ion in long-standing nitrate solutions was found to be Pu(IV). Current laboratory work pertains to initial hydrogen reduction experiments and exploratory pellet preparation, sintering, and characterization.

Installation of the denitration pilot plant was completed, and a series of shakedown runs were performed with uranyl nitrate solution alone (ANL-7755, pp. 40-44). The design production goal of 100 lb $UO_3/(hr)(ft^2)$ was met. Redesign and acquisition of equipment to meet the expected nuclear safety requirements for work with uranium-plutonium systems was carried out during the current quarter.

A. Laboratory Program

1. Reduction of UO_3-PuO_2

The denitration of uranyl nitrate-plutonium nitrate solutions produces UO_3-PuO_2, which must be reduced to UO_2-PuO_2 before pellets are made. Prior fluidized-bed experience[6] had indicated that reduction of UO_3 with hydrogen at ~550°C is feasible. Thermogravimetric (TGA) data[7] showed that in the reaction of UO_3 with hydrogen, reduction starts at approximately 400°C and is complete at 500°C.

Exploratory reduction experiments were carried out on UO_3-PuO_2 powder derived from drop-denitration experiments to provide UO_2-20 wt% PuO_2 for exploratory pellet fabrication and preliminary characterization tests. The UO_3-PuO_2 powder had been prepared by the dropwise addition of a nitrate solution (containing about 1.65M total U + Pu) into a quartz tube at 300°C.

Reduction was carried out at 550 and 500°C in a small stainless steel boat with approximately 6 g of UO_3-PuO_2 per experiment. The reaction time was 4 hr, and the hydrogen flow rate was 100-200 cm^3/min. Preliminary data indicate that reduction was on the order of 95% in both experiments. Further reduction studies await engineering denitration studies with uranyl nitrate-plutonium nitrate solutions.

2. Preparation of UO_2-PuO_2 Pellets

The purpose of these experiments was to determine whether $(U,Pu)O_2$ prepared by denitration and reduction could be fabricated into good quality pellets, i.e., whether the sintered pellets would have reasonable densities and homogeneous distribution of plutonium. Initial work has been to explore briefly the effects of fabrication conditions on density. In the first pellet preparation, UO_2-20 wt % PuO_2 derived by reduction at 550°C was pressed into 1/4-in.-dia pellets at 87,000 psi and sintered at 1650°F for 90 min. Sintering of this and other pellets was in an argon atmosphere. Physical measurement indicated that the pellets had a density of 84% of theoretical density (T.D.). Several additional pellets were fabricated to explore briefly the effects of fabrication conditions with the objective of achieving a higher pellet density.

Four additional UO_2-20 wt % PuO_2 pellets were made from -100 mesh powder produced by drop denitration at 300°C and hydrogen reduction at 500°C (rather than at 550°C as in the earlier work). Two of these pellets were pressed at 87,000 psi, and the other two were prepressed at 1500 psi pressure, granulated, and finally pressed at 87,000 psi. One pellet from each of the above pairs was sintered at 1650°C for 4 hr; the other two pellets were sintered at 1750°C for 90 min. The operating conditions and results for all pellet tests are summarized in Table I. Prolonged heating at 1650°C did not increase the density. The pellet which had been prepressed, granulated, pressed, and sintered at 1750°C had the highest density, 89% of theoretical. The density of the companion pellet, which had been pressed without granulation and sintered at 1750°C, was 83% of theoretical. Use of a lower temperature, 500°C instead of 550°C, for hydrogen reduction appeared to have no adverse effect on final pellet density.

From these preliminary results, we are optimistic that satisfactory fuel pellets can be prepared from this type of $(U,Pu)O_2$ by the selection of appropriate pelletizing and sintering conditions.

3. Examination of UO_2-PuO_2 Pellets

The $(U,Pu)O_2$ pellets were examined for composition, homogeneity, and structure.

a. Chemical Analysis

One pellet having a density of 84% of theoretical (Table I, Line 2) was used for analysis. One piece of this pellet was reserved for electron microprobe examination, and fragments of the second piece were analyzed for oxygen, uranium, and plutonium. The oxygen content was determined by vacuum fusion, and the uranium and plutonium concentrations were determined

Table I. Operating Conditions and Results of UO_2-PuO_2 Pellet Fabrication Tests

Run No.	Initial Powder Mesh Size	Prepressing Pressure (psi)	Granulated Powder Mesh Size	Pressing Pressure (psi)	Green Density (g/cm^3)	Sintering Temp. (°C)	Sintering Time (min)	Final Density (g/cm^3)	% of T.D.	Pellet Diam. (in.)	Pellet Length (in.)
87[a]	- [b]	None	c	87,000	6.2	1650	90	9.3	84	0.252	0.282
89A[d]	-100	None	c	87,000	5.9	1650	240	9.3	84	0.248	0.203
89A[d]	-100	∿1500	-45	87,000	6.1	1650	240	e	e	0.249	0.195
89B[d]	-100	None	c	87,000	5.9	1750	90	9.2	83	0.250	0.102
89B[d]	-100	∿1500	-45	87,000	6.2	1750	90	9.85	89	0.246	0.166

[a] The UO_2-PuO_2 powder was prepared by drop denitration at 300°C followed by hydrogen reduction at 550°C.

[b] Not measured.

[c] No granulation step used in these experiments.

[d] The UO_2-PuO_2 powder was prepared by drop denitration at 300°C followed by hydrogen reduction at 500°C.

[e] Not measured because the pellet was chipped and cracked.

amperometrically. The results, summarized below, are within the current Fast Flux Test Facility (FFTF) specifications.[8]

U (wt %)	70.78	70.70
	70.63	
Pu (wt %)	17.61	17.60
	17.60	
O (wt %)	11.64	11.74
	11.69	
	11.88	
Oxygen/Metal Atom Ratio		1.98

b. Electron Microprobe Examination

A section of a pellet was placed in a metallographic mount and polished suitably for electron microprobe examination. The final step was the deposition (by sputtering) of a 50Å coating of gold, which insures adequate conduction and prevents contamination of the equipment.

Bombardment by the electron beam (a 0.5-μm-dia beam in this case) results in characteristic X-rays of uranium and plutonium being emitted. Separate counting rates for uranium and plutonium were measured, and after correction for background, the uranium-to-plutonium counting ratio was calculated. The constancy of this counting ratio is one measure of pellet homogeneity. Twenty such measurements were made on various portions of the pellet. The data showed a spread of about 20%. An electron beam of the same size was also used in a scanning mode over many 8- by 10-μm areas and 80- by 100-μm areas for another series of measurements; no improvement in the dispersion of the data was observed. Nevertheless, these results are considered encouraging, since no spots or areas were found that contained only uranium or only plutonium. Scanning of the pellet across a diameter will be done next.

Analysis of the pellet also disclosed trace metal inclusions--tantalum and components of stainless steel (nickel, chromium, and iron peaks were noted). Subsequent examination indicated that contamination had occurred during sintering, and not during the denitration and reduction steps.

c. X-ray Examination

A lattice parameter of 5.4602Å for the pellet sample was measured. Only a single set of X-ray diffraction lines was in evidence, indicating the presence of a single oxide phase. This measured lattice parameter was compared with the lattice parameter predicted from a relationship between O/M and lattice parameter at a stated plutonium content, earlier observed by Schnizlein (ANL-7735, p. 76):

$$a_o = 6.1127 - 0.534\ (Pu) - 0.321\ (O/M) + 0.229\ (Pu)(O/M)$$

where a_o is the lattice parameter, $(Pu) = \frac{\%\ Pu}{\%\ Pu + \%\ U}$, and O/M is the oxygen to metal ratio. The value for a_o predicted by that relationship is 5.4610Å, which compares very favorably with the value obtained experimentally.

4. Solubility Limits for U-Pu Nitrate Solutions

A knowledge of the cosolubility of uranyl nitrate and plutonium nitrate in dilute nitric acid is important in relation to the feed composition selected for a fluid-bed denitration plant. The feed solution should be as concentrated as possible to increase the throughput of the fluid-bed denitration reactors. However, the feed solution should not be so concentrated that inadvertent crystallization of plutonium nitrate can occur because this could represent a criticality hazard. Since little crystallization data is available in the literature for uranyl nitrate-plutonium nitrate solutions with high plutonium contents, it is proposed to use cooling curves to determine the temperatures at which solutions of given compositions begin to crystallize. Several solutions of interest will be studied. From this information, the practical limits of concentration of U/Pu nitrate solutions for feeds in the denitration process will be selected.

The test procedure involves heating the test solution approximately 5°C above the temperature of first crystallization and allowing the solution to cool, with stirring. Meanwhile, the solution temperature is recorded. The onset of crystallization results in a change in the rate of cooling, giving a change in the slope of the curve when the recorded temperature is plotted against elapsed time. The crystallization point is taken as the intersection of the two lines drawn through the two segments of the cooling curves. The apparatus is singular in that the rate of cooling of the test solution (contained in a test tube projecting into a flask) is controlled by the flow rate of air cooled by dry ice located in the flask. Preliminary tests in which crystallization points were determined from cooling curves for uranyl nitrate solutions have demonstrated good agreement of experimental results with the published data on uranyl nitrate solutions.

In future work, cooling curves for appropriate solutions of uranyl nitrate-plutonium nitrate-nitric acid will be obtained.

B. Engineering Program

Work on the pilot plant for denitration (ANL-7735, p. 54) has consisted of the design and acquisition of new vessels and some piping modifications. Equipment was modified in accordance with a criticality hazards analysis of the pilot plant. The main changes concerned the feed make-up system, which includes a 4-in.-dia dissolver, a 3-in.-dia feed tank, and a 16-in.-dia feed storage tank. Borosilicate-glass Raschig rings are to be used as a fixed nuclear poison in the large-diameter vessel.

The assistance of ORNL in the criticality hazards analysis is acknowledged. Their Monte Carlo calculations, based on a rather conservative model which took no credit for ^{240}Pu or uranium dilution, showed a relatively low system reactivity, k_{eff}, near 0.7.

Installation work, including installation of the glovebox windows and pressure testing of the glovebox, is expected to be completed during the next quarter. Denitration work with plutonium systems can then be started.

III. IN-LINE ANALYSIS IN FUEL FABRICATION

(J. G. Schnizlein, T. Gerding, M. J. Steindler)

The development of rapid, precise, and accurate in-line nondestructive methods for the analysis of critical fuel properties will lower fuel fabrication costs for the large number of fuel pellets that will be processed in the LMFBR program. For this evaluation of analytical methods, the starting criteria selected are the specifications of preirradiation fuel properties (and the associated precisions) for the Fast Fuel Test Facility (FFTF) project. The fuel properties, specifications,[8] precisions, and acceptable methods of measurement[9] for the Fast Flux Test Facility (FFTF) were discussed in an earlier quarterly report (ANL-7735, pp. 59-66). As additional information on the relationship between fuel properties and fuel performance is obtained from irradiation experiments, more realistic and possibly less rigorous specifications for fuel properties are expected.

The fuel for the first commercial FBR is expected to be uranium-plutonium oxide. Two fuel properties have been selected for initial study because their determination is necessary in every conceivable fabrication procedure: plutonium/uranium (Pu/U) ratio and oxygen/metal ratio in uranium-plutonium oxide. A literature study indicating that oxygen/metal ratio can be determined by measurement of lattice parameters is described in ANL-7735, pp. 65, 71-80.

A. Plutonium/Uranium Ratio in Fuel

The most rigorous specification on plutonium content for FFTF fuel is for a core zone that must have an average plutonium content of 20.0 $\pm$ 0.1%. This imposes a precision of $\pm$0.5%, which is not routinely achievable. X-ray fluorescence analysis is being evaluated as an in-line analytical method for determining Pu/U ratio in UO_2-PuO_2 fuel materials. X-ray fluorescence analysis is a sensitive, nondestructive method in which exciting radiation impinges on the sample and causes the emission of radiation that is characteristic of the elements present; by application of this method, uranium and plutonium concentrations can be determined rapidly and accurately enough to be practical at high fuel-production rates. In the experimental program to demonstrate the practicality of this analysis, not only the material effects but also the instrumental choices and sample presentation procedures are being defined.

Initial investigations are being done with ThO_2-UO_2 as a stand-in for UO_2-PuO_2 to avoid the hazards of handling plutonium. This substitution is practical because of the identical relationship of the atomic numbers of each pair of elements and thus of the relevant properties (see ANL-7726, pp. 141-142). Part of the data obtained with ThO_2-UO_2 will later be verified in experiments with UO_2-PuO_2.

1. Instrumental Considerations

The precision of X-ray fluorescence analysis is limited by counting statistics (ANL-7735, p. 71)--that is, precision is improved at higher total counts. If the time to reach a count corresponding to the desired

precision is decreased, the opportunity for in-line application will be improved, as will the accommodation to higher production rates. Equipment modifications are desired that will increase uranium and thorium count rates without increasing the background rate too much.

There are eight identified processes[10] in a flat-crystal spectrometer where a loss of fluorescence intensity can occur due to instrumental effects. The two greatest loss factors are the efficiency of X-ray production (fraction of the X-rays striking the sample and re-emitted) and the fraction of the radiation emerging from the two collimators. Typical values of these two factors are 3.7×10^{-3} and 1.6×10^{-5}, respectively. Data presented last quarter (ANL-7755, pp. 46-47) demonstrated that 20-mil slit widths in the collimators (instead of the usual 5-mil slit widths) give adequate resolution of the uranium and thorium peaks and also increase counting rates tenfold. At the observed counting rate for uranium of 7×10^3 cps, a counting time of 0.5 min is necessary to obtain a precision of $\pm 0.5\%$ at the 95% confidence level. If the thorium peak and background were then counted sequentially, the estimated total counting time for each pellet would be about 1 min. New counting equipment that is expected to have a capability of 10^5 cps has since been installed and is being calibrated.

Sample Presentation. A controlled and reproducible method of presentation of the sample to the exciting radiation is necessary for precise measurements in X-ray spectrometry. The initial experiments were performed using aluminum masks with holes of various diameters to define the area of the sample that would be irradiated. Either powdered oxide contained in a shallow glass dish or solid samples were supported beneath the mask in a conventional carrier (Fig. 3).

A sample holder of new design (Fig. 4) was constructed that provides reproducible loading. Samples of powder or pellets are loaded in the aluminum cup so that the surface of the powder or pellets is even with the cup rim. Use of this sample holder and loading procedure has resulted in the counting rate increasing by a factor of 1.5 and the background count (from scattered X-rays) decreasing by a factor of 3. Thereby, the analysis time has been decreased and precision improved.

With the new counting equipment and the new sample-presentation method, uranium count rates up to 1.8×10^4 cps can be measured for 20% UO_2-80% ThO_2 samples and count rates of about 9×10^4 cps for pure materials. Still to be determined are corrections for dead time and coincidence at count rates above 3×10^4 cps.

2. Material Effects

The fluorescence intensity of a characteristic radiation is influenced by two kinds of matrix effects--absorption and enhancement. To attain the required precision in the analysis of solid oxide as powder or pellets, absorption and enhancement must be proved to be either insignificant or predictable.

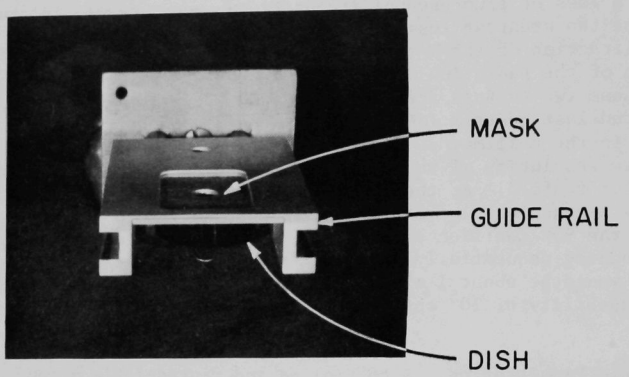

Fig. 3. Sample Carrier

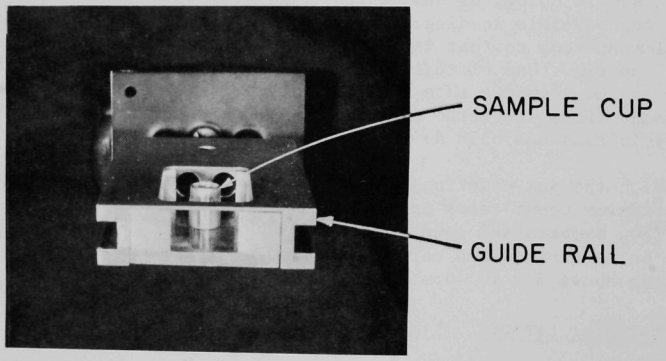

Fig. 4. Sample Holder

Absorption includes the effects of scattering from the surface, voids, and crystallites, as well as absorption described by the mass absorption coefficients of the elements present. Enhancement (or secondary fluorescence) occurs when the characteristic radiation from one component element has enough energy to excite the characteristic radiation of the element being measured. This occurs in uranium-plutonium oxides because PuLα excites ULα. In thorium-uranium oxides, ULα excites ThLα.

Normally, quantitative analysis by a fluorescence technique requires a set of standards covering the ranges of variables of interest, such as composition (element concentration and matrix content), density, crystallite size, and absorption coefficients. Criss and Birks[11] have formulated calculational methods whereby X-ray fluorescence intensities can be calculated from fundamental parameters. Computer calculations should greatly decrease the number of standards necessary by allowing some prediction of signal losses due to material effects.

Experimental work is required with samples having a range of plutonium contents to demonstrate whether the necessary precision can be attained despite variations in powder properties, such as particle size, bulk density, and O/M ratio.

a. Uranium Content of UO_2-ThO_2

Measurements of the intensity of the Lα emission line from uranium and thorium are being determined for mixtures of 10, 15, 20, 25 and 30 wt % UO_2-ThO_2 powder. The mixtures were prepared from pure ThO_2 and from UO_2 that had been reduced from NBS U_3O_8. Thorium, uranium, and oxygen contents of each of the pure oxides were verified by analysis.

b. Particle Size Effects

The influence of particle size is being evaluated in preliminary work by measuring ULα emission from samples of arc-fused UO_2. These samples had been sieved and separated into three fractions, <44 μm, 177-500 μm, and 500-1000 μm. The intensity of the ULα line for each fraction was compared with that for a standard (<44-μm UO_2 prepared from NBS U_3O_8). The ratios and the standard count rates for various irradiation experiments are presented in Table II. The count-rate ratios for two large-particle UO_2 samples to NBS UO_2 were each ∿0.7. Apparently, fluorescence intensity decreases at particle sizes greater than 44 μm. Further study will be required to determine the extent to which this effect interferes with the precision of analysis.

B. Conclusions

A procedure for determining U/Pu ratio by X-ray fluorescence analysis is being developed. This nondestructive analysis can be performed rapidly enough to be practical for large-scale processing.

Table II. Influence of Particle Size of Arc-Fused UO_2 on Emission Intensity

Experiment[a]	Standard[b,c] (cps)	Ratio of Count Rate of Fraction to Count Rate of Standard		
		<44 μm	177-500 μm	500-1000 μm
I	83000	0.98	0.69	0.73
II	73000	1.00	0.71	0.75
III	3057 ± 49	-	0.693	0.694
IV	1792 ± 13	-	0.712	-

[a] W target at 59 kVp, 41 mA

I 20-mil collimators, integral count mode
II 20-mil collimators, differential count mode
III 5-mil collimators, differential count mode
IV Filtered through 1-mil Sn foil, 5-mil collimator, differential count mode

[b] Standard used was <44-μm (-325 mesh) UO_2 reduced from NBS U_3O_8.

[c] The reasons for the difference between count rates in integral mode and count rates in the differential mode are not entirely clear and are being studied. Standard count rate is uncorrected for dead time.

IV. ADAPTATION OF CENTRIFUGAL CONTACTORS IN LMFBR FUEL PROCESSING

(G. Bernstein, J. Lenc, N. Quattropani)

The performance characteristics of centrifugal contactors during plutonium purification (plutonium-isolation steps) in the Purex-type solvent extraction of LMFBR fuel material are being investigated. The feed streams to the plutonium-isolation steps will contain high concentrations of plutonium. The hazard of nuclear incidents in these steps will be controlled by using a geometrically favorable design, i.e., by specifying a favorable diameter. Other expected advantages of centrifugal contactors are reduced radiation damage to solvent as a result of brief residence time in the contactor and improved ease of operation (including rapid flushout at the end of a processing campaign).

A stainless steel contactor is being fabricated here that has the same general configuration as Savannah River (SR) centrifugal contactors now in use for first-cycle solvent extraction of production-reactor fuels. In this design, a hollow cylindrical rotor (attached to a shaft that penetrates the top of the contactor) spins inside a cylindrical stator (i.e., casing). A mixing paddle, mounted on the same shaft as the rotor, spins inside a mixing chamber below the rotor. Organic and inorganic streams enter at the bottom of this chamber. The mixing paddle also acts as a pump, and the mixed phases pass through a nozzle into the bottom of the rotor. The two phases are separated by centrifugal force as the mixture flows upward through the rotor. The separated phases are discharged over weirs and through separate ports into collecting rings. The centrifugal contactors being studied here, which have small diameters in comparison with SR contactors, also have increased bowl lengths and increased operating speeds to maintain a relatively high capacity.

Fabrication of the stainless steel contactor (ANL-7735, p. 84) is nearing completion, with only dynamic balancing of the rotor and assembly of components still to be done. The stator ID is 4 3/4 in.; the hollow rotor has a 4-in. ID, a 0.1-in.-thick wall and a 12-in.-long settling zone. The contactor is designed to operate at speeds up to about 3600 rpm and is expected to have a capacity of at least 10 gpm.

This unit is designed to be convertible into an annular mixer unit by removing the paddle and mixing chamber. Feed streams then enter through the sides of the stator, are mixed by skin friction as the phases flow down through the annulus between the rotor and stator, and are separated in the manner described above. Such a design is being investigated in anticipation that it will offer the advantage of mechanical simplicity in comparison to the SR design.

Pending completion of the stainless steel contactor, some preliminary tests were conducted in an annular mixer made of plastic to evaluate performance characteristics. The sizes of the plastic model and stainless steel contactor are approximately the same. Details of the design of the plastic unit are shown and described in the previous report in this series, ANL-7755, pp. 51-53. Also reported were test results indicating that throughputs of $\sim$10 gpm could be obtained at rotor speeds up to $\sim$1650 rpm. Results of mixing

power tests suggested that intensive phase contact is developed in the annular space of this contactor.

A. Phase Mixing and Separation

More recently with the plastic contactor installed in a test facility (ANL-7735, p. 87), tests have been made to evaluate phase-separating capacity.[12] These tests initially employed 0.1M HNO_3 as the aqueous phase and Ultrasene (refined kerosene) as the organic phase. These tests showed that, for flow rates of aqueous and organic phases of about 2 gpm each and rotor speeds of about 1800 rpm, phases were well mixed. However, the aqueous output stream contained a high concentration (~25%) of organic phase. Higher rotor speeds did not change the extent of contamination. At very low organic phase flow rates (<0.5 gpm) and aqueous flow rates between 3 and 4 gpm, the aqueous output stream contained between 1.6 and 2.5% organic phase in a test when rotor speeds were between 1500 and 2200 rpm. The organic phase output stream was uncontaminated in all tests.

Several possible explanations for the contamination of the aqueous output stream were investigated. Neither overmixing nor inadequate phase separation appeared to be a valid cause. Although mixing power input in the annulus had earlier been shown to be high, it was observed that when the rotor was stopped, separation of the mixed phases in the annulus took place in less than 30 sec. Accordingly, separation in the rotor should have been adequate under a centrifugal force greater than 200 times the force of gravity.

Another possibility was that the emulsion band at the interface between the settled aqueous and organic phases at the top of the rotor was too close to the aqueous phase baffle. The position in the rotor of the interface was calculated,[13] based on weir dimensions, flow rates, and phase densities. The location of the emulsion band was calculated to be where desired--between the organic weir and the aqueous phase underflow baffle. However, it was thought possible that the interface was in fact too close to the aqueous phase baffle. Since the plastic contactor is not equipped with an air-controlled aqueous weir, the emulsion band could be shifted toward the organic weir only by increasing the density of the aqueous phase. Accordingly, the aqueous phase was made about 1M in aluminum nitrate (sp gr, 1.136). Neither this change in density nor a further increase in specific gravity to 1.2 had a significant effect on the extent of contamination of the aqueous phase output stream with organic phase.

In view of the above performance, it is presently believed that organic phase contamination of the aqueous phase output stream is due to leakage through cracks in the weir tube for the organic phase. This tube is relatively thin (1/16 in.). Examination showed fine hairline cracks that may penetrate the wall and provide a channel for the organic liquid under centrifugal stress. Separated organic phase could flow through these cracks into the aqueous phase discharge passage. The design of the stainless steel unit currently being assembled would preclude this material defect. Since most of the goals sought by operation of the plastic unit were reached no further runs with the plastic contactor are planned. Additional testing of the annular mixing concept will be made in the stainless steel contactor.

REFERENCES

1. M. Hansen and K. Anderko, Constitution of Binary Alloys, McGraw-Hill, New York (1958), p. 1060.

2. The maximum pressure expected in reference Atomics International LMFBR fuel elements at 600°C is 52 atm.

3. D. E. Ferguson et al., Chemical Technology Division Annual Progress Report for Period Ending May 31, 1970, USAEC Report ORNL-4572, pp. 53-54 (October 1970).

4. A. R. Irvine, private communications (May 1970, September 1970, and December 1970).

5. A. A. Jonke, E. J. Petkus, J. W. Loeding, and S. Lawroski, Nucl. Sci. Eng. 2, 303 (1957)

6. S. M. Stoller and R. B. Richards, eds., Reactor Handbook, Vol. II, 2nd Ed., Interscience Publishers, New York (1961), p. 361.

7. G. Berggren and A. Brown, "The Influence of Oxide Additions on the Reduction of UO_3 and U_3O_8 as Measured by DTA and TGA," in Proceedings of Second International Conference on Thermal Analysis, 1968, Vol. 2, R. F. Schwenker and P. D. Garn, eds., Academic Press, New York (1969), p. 881.

8. C. A. Strand, Pacific Northwest Laboratory, private communication (February 1969).

9. Analytical Chemistry Methods in Support of Driver Fuel Fabrication, USAEC Report BNWL-1024 (October 1968).

10. H. A. Liebhafsky, X-ray Absorption and Emission in Analytical Chemistry, John Wiley & Sons, New York (1960), p. 27.

11. J. W. Criss and L. S. Birks, Anal. Chem. 40, 1080 (1968).

12. Product of Atlantic Richfield Co.

13. D. S. Webster, C. L. Williamson, and J. F. Ward, Flow Characteristics of a Circular Weir in a Centrifugal Field, USAEC Report DP-371 (June 1961).

B